JPEDAV (2006) 27:477-481
DOI: 10.1361/154770306X132010
1547-7037/$19.00 ©ASM International

Observation of Incongruent Melting in $Cu_{10}Hf_7$

R.H. Woodman, B.R. Klotz, and L.J. Kecskes

(Submitted January 24, 2006; in revised form June 14, 2006)

Differential thermal analysis, scanning electron microscopy, and x-ray microanalysis are used to show that the intermetallic compound $Cu_{10}Hf_7$, previously reported as melting congruently at 1025 °C, melts incongruently to $CuHf_2$ and a Hf-Cu liquid at that temperature. A eutectic point previously reported at 43.6 at.% Hf and 980 °C does not exist.

Keywords binary system, copper, differential thermal analysis, electron probe microanalysis, equilibrium diagram, experimental study, hafnium

1. Introduction

Equilibrium relations in the binary Hf-Cu system have been investigated or assessed multiple times since the early 1960s.[1-3] The most recent reference[1] indicates $Cu_{10}Hf_7$ melts congruently at 1025 °C and forms eutectic mixtures with Cu_8Hf_3 and $CuHf_2$ (Fig. 1). The eutectic with Cu_8Hf_3 is at 38.6 at.% Hf and melts at 970 °C. The eutectic with $CuHf_2$ is reportedly at 43.6 at.% Hf and melts at 980 °C. The authors have observed evidence that $Cu_{10}Hf_7$ in fact melts incongruently at 1025 °C, forming $CuHf_2$ and a liquid and that the eutectic with $CuHf_2$ does not exist.

R.H. Woodman and **B.R. Klotz,** Dynamic Science, Inc.; and **L.J. Kecskes,** Weapons and Materials Research Directorate, Army Research Laboratory, AMSRD-ARL-WM-MB, Aberdeen Proving Ground, MD, 21005-5069. Contact e-mail: robw39@mindspring.com.

2. Experimental Procedure

Alloyed Hf-Cu ingots were prepared by melting mixtures of the elemental metals in an electric arc furnace with a titanium-gettered argon atmosphere. Prior to melting, both metals were treated in an aqueous solution of nitric and hydrofluoric acids, rinsed in ethanol, and dried. Each ingot was flipped and remelted a minimum of six times. Nominal compositions of the ingots are listed in Table 1.

Differential thermal analysis (DTA) was conducted using a Netzsch Simultaneous Thermal Analyzer 409C (Netzsch Instruments, Inc., Burlington, MA) fitted with S-type thermocouples. Differential thermal analysis samples were blanketed in a flowing argon atmosphere and contained in graphite crucibles. Heating or cooling rates during data collection were 10 K/min. To establish good thermal

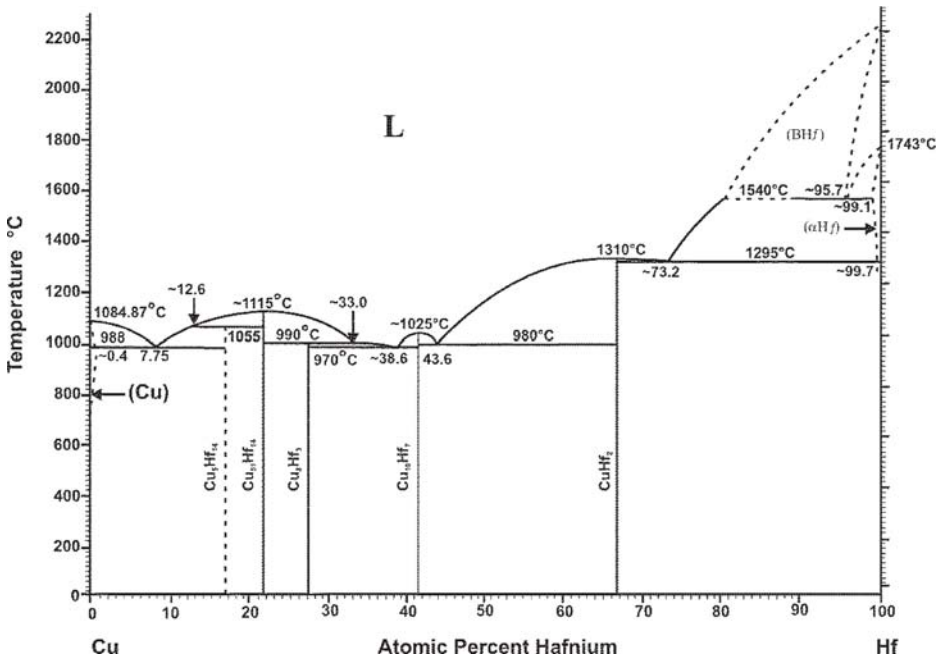

Fig. 1 Hafnium-copper phase diagram from Ref 1

contact between crucible and sample, samples were melted and resolidified in the DTA furnace prior to the analysis scan.

Backscattered electron micrographs were prepared using samples that had been melted and cooled in the DTA. For the first five samples in the table, the DTA was cooled at 10 K/min. The two highest-Hf-content samples were furnace cooled (the power was switched off at the peak temperature, and the furnace cooled on its own). Mounted microscopy

Table 1 Results of standardless analysis of x-ray spectra from microstructures

Sample	Area (a)	High BS (b)	Medium BS (c)	Low BS (d)	Eutectic (e)
$Hf_{38.6}Cu_{61.4}$	$Hf_{36}Cu_{64}$	N/A	N/A	N/A	N/A
$Hf_{40}Cu_{50}$	N/A	N/A	N/A	N/A	N/A
$Hf_{41.2}Cu_{58.8}$	$Hf_{41}Cu_{59}$	$Hf_{66}Cu_{34}$	$Hf_{42}Cu_{58}$	$Hf_{25}Cu_{75}$	N/A
$Hf_{43.6}Cu_{56.4}$	$Hf_{42}Cu_{58}$	$Hf_{63}Cu_{37}$	$Hf_{40}Cu_{60}$	N/A	N/A
$Hf_{50}Cu_{50}$	$Hf_{53}Cu_{47}$	$Hf_{66}Cu_{34}$	$Hf_{42}Cu_{58}$	$Hf_{24}Cu_{76}$	$Hf_{31}Cu_{69}$
$Hf_{55}Cu_{45}$	$Hf_{53}Cu_{47}$	$Hf_{64}Cu_{36}$	$Hf_{41}Cu_{59}$	$Hf_{27}Cu_{73}$	$Hf_{31}Cu_{69}$
$Hf_{60}Cu_{40}$	$Hf_{58}Cu_{42}$	$Hf_{65}Cu_{35}$	$Hf_{42}Cu_{58}$	$Hf_{29}Cu_{71}$	$Hf_{32}Cu_{59}$

(a) Area means a spectrum collected from the entire area of the associated micrograph and gives an indication of the error of the quantitative analysis. (b) High BS refers to a spectrum collected from the phase of highest backscatter intensity, i.e., the most dense phase. (c) Medium BS and (d) Low BS refer to spectra collected from the lower-density phases. (e) eutectic refers to a spectrum from an area with eutectic microstructure.

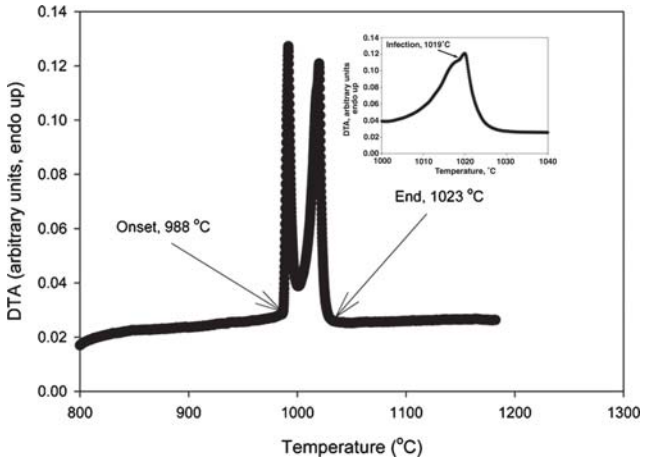

Fig. 2 DTA trace from $Hf_{41.2}Cu_{58.8}$ ($Cu_{10}Hf_7$)

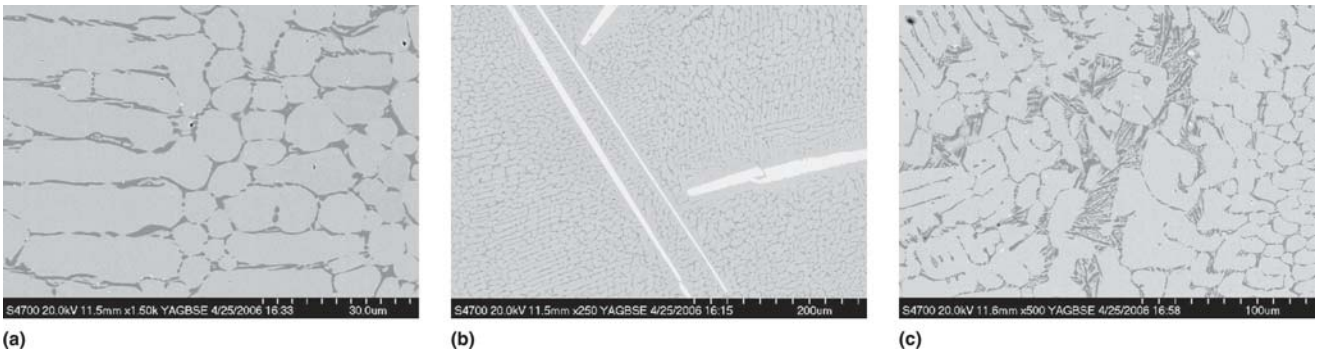

Fig. 3 Backscatter SEM of $Hf_{41.2}Cu_{58.8}$ ($Cu_{10}Hf_7$). The light phase is $CuHf_2$, the medium-contrast phase is $Cu_{10}Hf_7$, and the dark phase is Cu_8Hf_3. Most of the microstructure of the sample appears as 3 (a), but there are regions where $CuHf_2$ can be seen (b) or where there is a greater fraction of the Cu_8Hf_3-$Cu_{10}Hf_7$ eutectic (c).

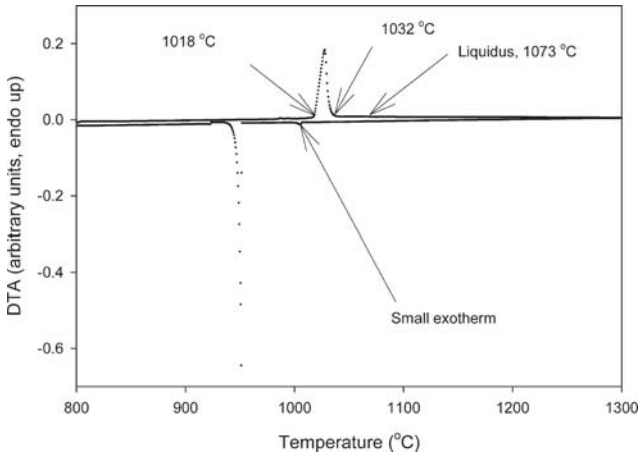

Fig. 4 Differential thermal analysis trace from $Hf_{43.6}Cu_{56.4}$ (reported eutectic composition)

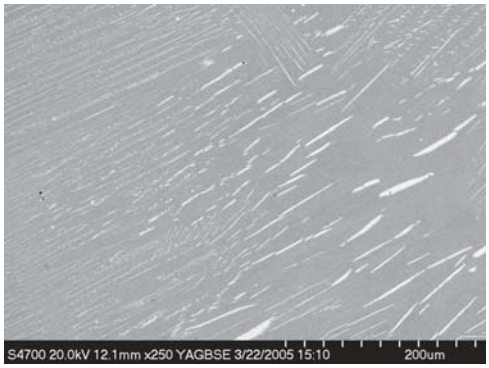

Fig. 5 Backscatter SEM of $Hf_{43.6}Cu_{56.4}$ ($Cu_{10}Hf_7$-$CuHf_2$ eutectic composition). The light phase is $CuHf_2$, the dark phase is $Cu_{10}Hf_7$.

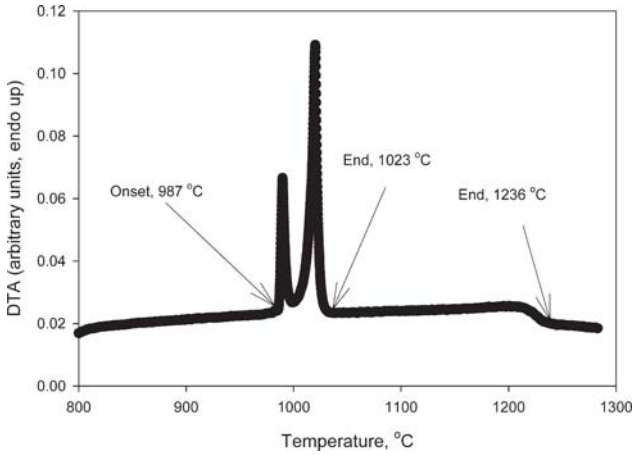

Fig. 6 DTA trace of $Hf_{50}Cu_{50}$ at 10 °C/min

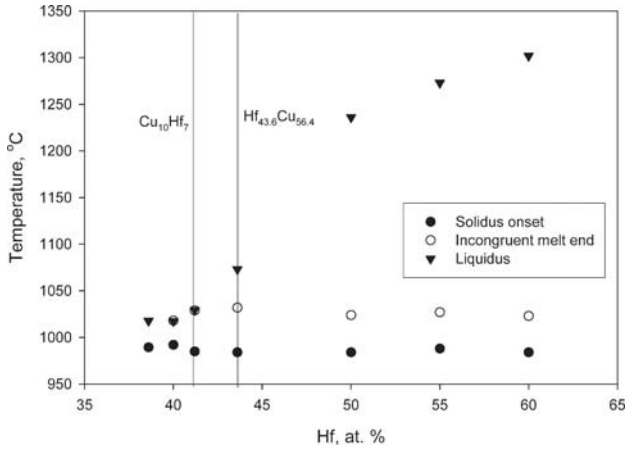

Fig. 7 Plot of solidus onset, intermediate peak end point, and liquidus end temperatures from the DTA traces for all samples in Table 1

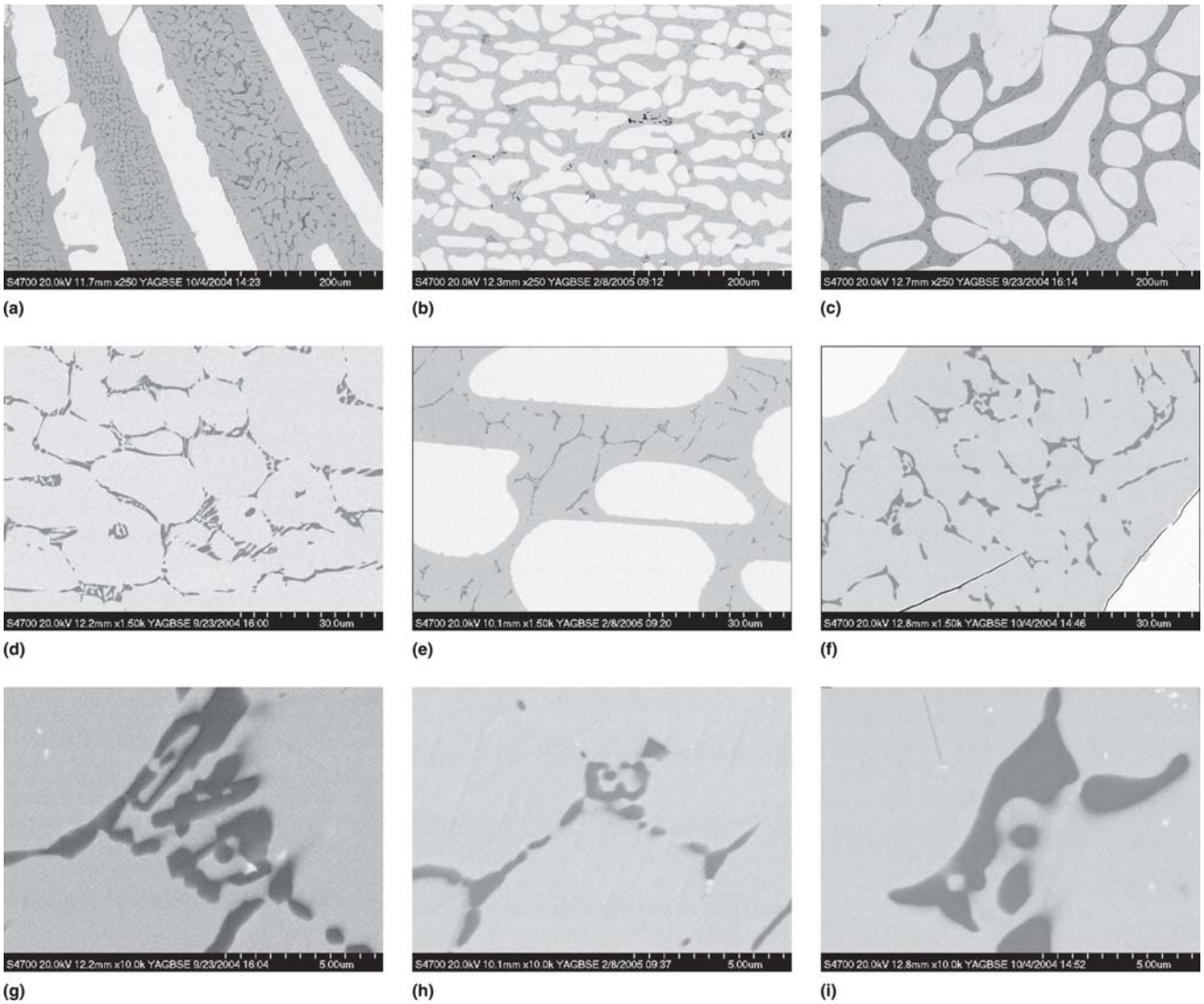

Fig. 8 Backscatter SEM images of (left to right) $Hf_{50}Cu_{50}$, $Hf_{55}Cu_{45}$, and $Hf_{60}Cu_{40}$ at (top to bottom) 250×, 1500×, and 10,000×. The light phase is $CuHf_2$; the medium-contrast phase is $Cu_{10}Hf_7$, and the dark phase is Cu_8Hf_3.

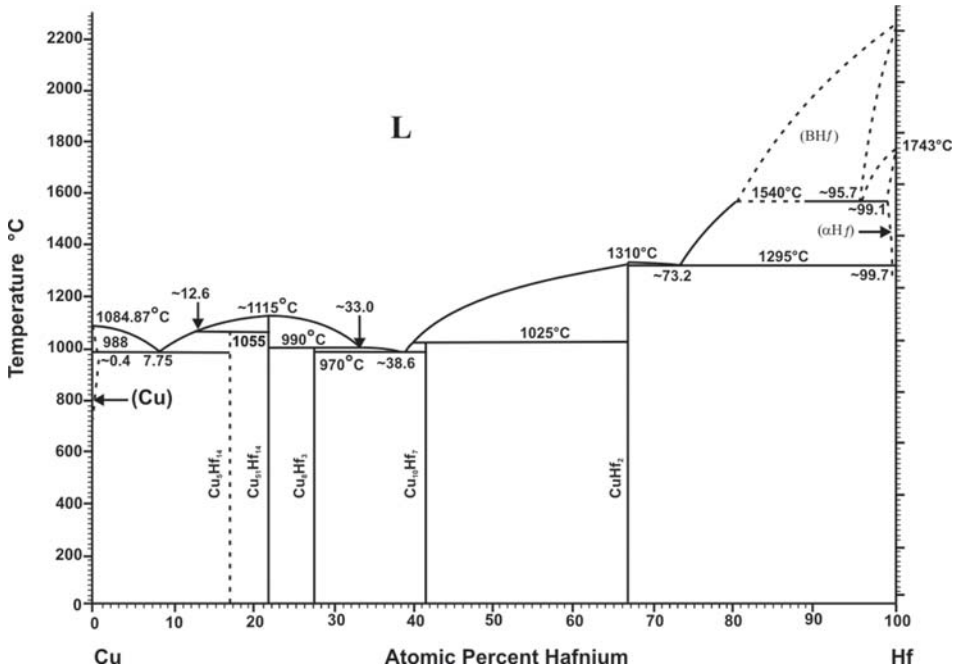

Fig. 9 Hafnium-copper diagram revised to reflect the incongruent melting of $Cu_{10}Hf_7$. The composition of the peritectic point is not known.

samples were polished to a 1 μm finish. The microscope was a Hitachi S-4700 (Hitachi High Technologies America, Schaumberg, IL) equipped with an yttrium-aluminum-garnet backscatter detector. Quantitative microanalysis of the x-ray spectrum from grains of each phase was performed using the standardless quantitative analysis feature of the EDAX Genesis system (EDAX Inc., Mahwah, NJ).

3. Results and Discussion

Figure 2 displays the DTA trace for the nominally $Hf_{41.2}Cu_{58.8}$ ($Cu_{10}Hf_7$) sample. There are three endotherms in the DTA trace, although two are convoluted in the second peak (Fig. 2 inset). Figure 3 displays microstructures from this sample, while Table 1 displays microanalysis results. Three phases are present in the microstructure—$CuHf_2$, $Cu_{10}Hf_7$, and Cu_8Hf_3. If the current phase diagram is accurate, one would expect at most two phases—$Cu_{10}Hf_7$ and, depending on the actual stoichiometry of the sample, eutectic regions containing either $CuHf_2$ or Cu_8Hf_3, but not both.

Figure 4 displays the DTA trace for the nominally $Hf_{43.6}Cu_{56.4}$ sample, the reported $Cu_{10}Hf_7$-$CuHf_2$ eutectic composition. Figure 5 displays the microstructure; microanalysis results are in Table 1. Initially, the DTA peak and the microstructure appear to be consistent with a eutectic. The DTA peak appears sharp and symmetric, and the microstructure is a finely divided two-phase mixture. The solidus (1018 °C) and apparent liquidus (1032 °C) are above the 980 °C melting temperature in the assessed diagram, but otherwise the evidence appears to be consistent with a eutectic. Examination of the cooling curve of the DTA scan reveals that the liquidus temperature is obscured by noise in the heating curve, but is still detectable with close scrutiny. The cooling curve reveals a small exotherm at 1007 °C. Close examination of the heating curve reveals a small change in slope at ~1073 °C. Although the small change in slope is not sufficient to assign 1073 °C as the liquidus temperature, the corroborating evidence of the cooling curve and the microstructure support this interpretation. A liquidus of 1073 °C would mean that both phases undercooled by about the same amount, 70 to 80 °C. The microstructure reveals that the volume fraction of $CuHf_2$ was low compared with $Cu_{10}Hf_7$, so its thermal signature on melting would be small.

More definitive evidence that $C_{10}Hf_7$ melts incongruently can be found in the results from the higher-Hf-content samples. Figure 6 displays the DTA trace for $Hf_{50}Cu_{50}$. There are three endotherms—sharp peaks at 987 and 1023 °C, and an event that begins at 1023 °C and concludes at 1236 °C. The DTA traces of the remaining samples—$Hf_{55}Cu_{45}$ and $Hf_{60}Cu_{40}$—are similar, with the relative sizes of the peaks changing and the liquidus rising with Hf content.

Figure 7 displays a plot of the temperatures associated with each peak for all samples. As the Hf content increases, the liquidus rises. However, there are still three endothermic events for each sample with a Hf content greater than 50 at.%. This can be correlated with the microstructure to give a clearer indication that $Cu_{10}Hf_7$ melts incongruently.

Figure 8 illustrates the microstructures of these samples. There are three phases, each corresponding to a DTA endotherm. Table 1 displays the results of the microanalysis of these samples. From the density of the phases, the micro-

probe results, and the morphology of the microstructure, it is evident that $CuHf_2$ is the primary phase. Assuming the sample was cooled slowly enough to achieve equilibrium, and if the assessed phase diagram is accurate, then the microstructures would exhibit two phases—a $CuHf_2$ primary phase and a eutectic mixture of $Cu_{10}Hf_7$ and $CuHf_2$. Instead, Fig. 8 exhibits three phases—a $CuHf_2$ primary phase, a secondary phase of $Cu_{10}Hf_7$, and a eutectic mixture of $Cu_{10}Hf_7$ and Cu_8Hf_3.

Examination of the morphology of the $Cu_{10}Hf_7$ secondary phase reveals that it appears to have nucleated preferentially on the $CuHf_2$ primary particles, and that the peritectic material is isolated from the $CuHf_2$ particles. This is consistent with the peritectic solidification process described in textbooks.[4] Because $Cu_{10}Hf_7$ melts incongruently, for the reaction to go to completion the components of the isolated peritectic liquid would need to diffuse through the $Cu_{10}Hf_7$ phase and react with decomposing $CuHf_2$ to form $Cu_{10}Hf_7$. Because this process rarely goes to completion in practice,[4] isolated pockets of liquid with a peritectic composition remain. Further cooling leads to the crystallization of Hf-rich crystals of $Cu_{10}Hf_7$, shifting the remaining liquid composition to the eutectic point. This liquid solidifies last as a eutectic mixture of Cu_8Hf_3-$Cu_{10}Hf_7$ phases, as is the case in Fig. 8. The DTA and microstructural evidence are both consistent with $Cu_{10}Hf_7$ melting incongruently. Figure 9 shows the revised phase diagram.

4. Conclusions

Contrary to earlier reports, $Cu_{10}Hf_7$ has been observed to be an incongruently melting compound, decomposing to $CuHf_2$ and liquid at 1025 °C. The composition of the peritectic point between $Cu_{10}Hf_7$ and the $Cu_{10}Hf_7$-Cu_8Hf_3 eutectic remains to be determined.

Acknowledgments

The authors would like to thank Ms. Minna Kim and Mr. George Dewing for their assistance in preparing samples for this study. The authors would also like to thank Ms. Amy Kehring for her assistance with graphics.

References

1. H. Okamoto, *Desk Handbook: Phase Diagrams for Binary Alloys,* ASM International, 2000, p 298
2. P.R. Subramanian and D.E. Laughlin, Copper-Hafnium, *Binary Alloy Phase Diagrams,* 2nd ed., T.B. Massalski, Ed., ASM International, 1990, p 1416-1419
3. P.R. Subramanian and D.E. Laughlin, The Cu-Hf System, *Bull. Alloy Phase Diagrams,* 1988, **9**(1), p 51-56
4. D.A. Porter and K.E. Easterling, *Phase Transformations in Metals and Alloys,* 2nd ed, Chapman and Hall, New York, 1992, p 231-233